Molecular and Cellular Biology

Macrophage Glucose-6-Phosphate Dehydrogenase Stimulates Proinflammatory Responses with Oxidative Stress

Mira Ham, Joo-Won Lee, A Hyun Choi, Hagoon Jang, Goun Choi, Jiyoung Park, Chisayo Kozuka, Dorothy D. Sears, Hiroaki Masuzaki and Jae Bum Kim

Mol. Cell. Biol. **2013, 33(12):2425. DOI: 10.1128/MCB.01260-12.**
Published Ahead of Print 9 April 2013.

MCB
Journals.ASM.org

Macrophage Glucose-6-Phosphate Dehydrogenase Stimulates Proinflammatory Responses with Oxidative Stress

Mira Ham,[a] Joo-Won Lee,[a] A Hyun Choi,[a] Hagoon Jang,[a] Goun Choi,[a] Jiyoung Park,[a] Chisayo Kozuka,[c] Dorothy D. Sears,[d] Hiroaki Masuzaki,[c] Jae Bum Kim[a,b]

School of Biological Sciences, Institute of Molecular Biology and Genetics, National Creative Research Initiatives Center for Adipose Tissue Remodeling,[a] and Department of Biophysics and Chemical Biology,[b] Seoul National University, Seoul, South Korea; Division of Endocrinology, Diabetes and Metabolism, Hematology and Rheumatology, Graduate School of Medicine, University of the Ryukyus, Nishihara, Okinawa, Japan[c]; Division of Endocrinology and Metabolism, Department of Medicine, University of California, San Diego, San Diego, California, USA[d]

Glucose-6-phosphate dehydrogenase (G6PD) is a key enzyme that regulates cellular redox potential. In this study, we demonstrate that macrophage G6PD plays an important role in the modulation of proinflammatory responses and oxidative stress. The G6PD levels in macrophages in the adipose tissue of obese animals were elevated, and G6PD mRNA levels positively correlated with those of proinflammatory genes. Lipopolysaccharide (LPS) and free fatty acids, which initiate proinflammatory signals, stimulated macrophage G6PD. Overexpression of macrophage G6PD potentiated the expression of proinflammatory and pro-oxidative genes responsible for the aggravation of insulin sensitivity in adipocytes. In contrast, when macrophage G6PD was inhibited or suppressed via chemical inhibitors or small interfering RNA (siRNA), respectively, basal and LPS-induced proinflammatory gene expression was attenuated. Furthermore, macrophage G6PD increased activation of the p38 mitogen-activated protein kinase (MAPK) and NF-κB pathways, which may lead to a vicious cycle of oxidative stress and proinflammatory cascade. Together, these data suggest that an abnormal increase of G6PD in macrophages promotes oxidative stress and inflammatory responses in the adipose tissue of obese animals.

Obesity is a key risk factor for metabolic diseases, including hyperlipidemia, atherosclerosis, hypertension, insulin resistance, and type 2 diabetes (1, 2). During the past few decades, the mechanisms linking obesity to metabolic diseases have been intensively investigated, and accumulating evidence suggests that the adipose tissue of the obese exhibits chronic and low-grade inflammation, which is closely associated with metabolic dysregulation (3). In obesity, adipose tissue macrophages (ATMs) produce various proinflammatory cytokines and chemokines, such as tumor necrosis factor alpha (TNF-α) (4), interleukin-6 (IL-6), and monocyte chemoattractant protein 1 (MCP-1), whose elevation mediates metabolic dysregulation and insulin resistance (5–8). Accordingly, MCP-1 and CCR2 (MCP-1 receptor) knockout mice are protected from insulin resistance and have a decreased number of ATMs, suggesting that proinflammatory cytokines and chemokines are essential for the recruitment of ATMs and disruption of insulin sensitivity in obesity (6, 7).

Macrophages are the major effector cells that constitute the innate immune system and perform multiple roles, such as phagocytosis, secretion of cytokines and chemokines, and antigen presentation, when they recognize pathogens or cellular debris (9). These responses are mediated by the generation of reactive oxygen/reactive nitrogen species (ROS/RNS), such as superoxide ($\cdot O_2^-$), hydrogen peroxide (H_2O_2), nitric oxide ($\cdot NO^-$), and peroxynitrite ($ONOO^-$) (10), which play a key role in killing bacteria and delivering signals as second messengers (11). ROS and RNS participate in various signaling pathways by activating and phosphorylating mitogen-activated protein kinases (MAPKs), including extracellular signal-regulated protein kinase (ERK), c-Jun N-terminal kinase (JNK), and p38 MAPK isoforms. In addition, ROS contributes to the regulation of gene expression through modulation of several transcription factors, including NF-κB (12), c-Fos, and c-Jun (13), which are responsible for the expression of proinflammatory cytokines, chemokines, and signaling components.

Endogenous ROS is generated by both nonenzymatic and enzymatic reactions (14). Mitochondria are a major source of nonenzymatic ROS production (15). However, in macrophages, abundant ROS is generated by enzymatic reactions of multicomponent NADPH oxidase 2 (NOX2) (16). Upon phagocytosis and/or various stimuli, NOX2 transfers 1 electron from NADPH to oxygen to generate a superoxide anion. In addition, endogenous nitric oxide is enzymatically produced by inducible nitric oxide synthases (iNOS) through the oxidation of L-arginine in the presence of oxygen and NADPH (14). Because NOX2 and iNOS require NADPH in common, sufficient NADPH is necessary to produce cellular ROS and RNS in macrophages.

Glucose-6-phosphate dehydrogenase (G6PD), the first and rate-limiting enzyme of the pentose phosphate pathway (PPP), is a key enzyme in the generation of cytosolic NADPH. G6PD participates in multiple metabolic pathways, such as reductive biosynthesis, regulation of oxidative stress, and cellular growth. We previously demonstrated that G6PD is highly expressed in the adipocytes of obese animals, and its overexpression in adipocytes impairs lipid homeostasis and adipocytokine expression, resulting

Received 12 September 2012 **Returned for modification** 15 October 2012
Accepted 1 April 2013
Published ahead of print 9 April 2013
Address correspondence to Jae Bum Kim, jaebkim@snu.ac.kr.
Supplemental material for this article may be found at http://dx.doi.org/10.1128/MCB.01260-12.

doi:10.1128/MCB.01260-12

in insulin resistance (17). We also showed that increased adipocyte and pancreatic β-cell G6PD is closely associated with oxidative stress in the onset of metabolic disorders (18, 19). However, the functions of macrophage G6PD in pathophysiological conditions such as obesity have not been fully elucidated. Since oxidative stress is a critical factor in the regulation of macrophages' proinflammatory roles, we hypothesized that macrophage G6PD might be a crucial enzyme that affects cellular redox and inflammatory cascades in response to metabolic changes.

In the present study, we demonstrate that macrophage G6PD is involved in the proinflammatory responses, accompanied by oxidative stress. G6PD is highly expressed in ATMs, and its expression level is significantly higher in obese animals. In macrophages, G6PD stimulates the expression of ROS- and RNS-producing genes and increases the levels of inflammatory cytokines, including IL-6, IL-1β, MCP-1, and TNF-α, which attenuate insulin signaling in adipocytes. Furthermore, macrophage G6PD activates p38 MAPK and NF-κB, which are key regulators of oxidative stress and proinflammatory responses. Taken together, these data suggest that macrophage G6PD enhances oxidative stress and inflammatory signaling, which may lead to insulin resistance in the adipose tissue of obese animals.

MATERIALS AND METHODS

Animals. C57BL6/J mice were purchased from Central Lab Animal Inc. (Seoul, South Korea) and were housed in colony cages in a 12-h light/12-h dark cycle. After a minimum of 1 week for stabilization, the mice were fed a normal chow diet (NCD) or high-fat diet (HFD) for 10 weeks (Research Diets Inc., New Brunswick, NJ). Eight-week-old C57BLKS/J-*Lepr*^{db}/*Lepr*^{db} mice were obtained from Central Lab Animal Inc. (Seoul, South Korea). All animal procedures were in accordance with the research guidelines for the use of laboratory animals of Seoul National University.

Reagents and inhibitors. Dehydroepiandrosterone (DHEA), 6-aminonicotinamide (6-AN), lipopolysaccharide (LPS), *N*-acetyl-L-cysteine (NAC), hydrogen peroxide, NADPH (NADP, reduced), free fatty acid (FFA) (palmitic acid), SB 203580, PD 98059, and SP 600125 were purchased from Sigma (St. Louis, MO).

Cell culture. RAW 264.7 macrophages were purchased from the American Type Culture Collection (Manassas, VA). RAW 264.7 cells were grown in Dulbecco's modified Eagle's medium (DMEM) (HyClone, Logan, UT) supplemented with 10% fetal bovine serum (FBS), 100 U/ml penicillin, and 100 mg/ml streptomycin. Cells were maintained at 37°C in a humidified atmosphere containing 5% CO_2. 3T3-L1 preadipocytes were maintained in DMEM supplemented with 10% bovine calf serum. To differentiate 3T3-L1 cells, they were grown to confluence and stimulated with DMEM containing 10% fetal bovine serum, dexamethasone (1 μM), methylisobutylxanthine (520 μM), and insulin (167 nM) for 48 h. Then, the culture medium was exchanged for DMEM containing 10% fetal bovine serum and insulin (167 nM) for another 48 h, and 3T3-L1 cells were maintained with DMEM containing 10% fetal bovine serum.

Fractionation of mouse adipose tissues. To prepare stromal vascular cells (SVCs) from adipose tissue, mice were sacrificed. Gonadal fat pads were isolated and incubated in 30 ml of collagenase buffer (0.1 M HEPES, pH 7.4, 0.125 M NaCl, 50 mM KCl, 1.3 mM $CaCl_2$, 0.5 M glucose, 0.45 g bovine serum albumin [BSA], and 30 mg of collagenase) at 37°C for 40 min with shaking and shearing. Then, the treated tissues were filtered through 100-μm-pore-size nylon mesh to remove debris and centrifuged at 930 × *g* for 3 min. SVCs were obtained in the pellet. To remove red blood cells (RBCs), the pellet was incubated in RBC lysis buffer (1.7 M Tris, pH 7.65, and 0.16 M NH_4Cl) for 15 min. After RBC lysis, the SVCs were washed several times with phosphate-buffered saline (PBS).

Flow cytometry analysis. For macrophage G6PD analysis, SVCs were stained with CD11b (BD Bioscience, San Jose, CA) and F4/80 (eBioscience, San Diego, CA) monoclonal antibodies (MAbs) for 20 min at 4°C. After mild washing, SVCs were fixed and permeabilized with BD Cytofix/Cytoperm, following the manufacturer's instructions (BD Bioscience, San Jose, CA). G6PD antibody purchased from Abcam (Cambridge, United Kingdom) was used to stain intracellular G6PD. SVCs were analyzed using the fluorescence-activated cell sorting (FACS) CantoII instrument (BD Bioscience, San Jose, CA).

Isolation of peritoneal macrophages. Mice were stimulated by an intraperitoneal injection of a thioglycolate solution (3 ml per mouse) and kept under pathogen-free conditions for 3 days before peritoneal macrophage isolation. Total peritoneal macrophages were harvested by washing the peritoneal cavity with PBS containing 30 mM EDTA (8 ml per mouse). The peritoneal wash fluid was centrifuged, and the cells were suspended in RPMI 1640 medium (HyClone, Logan, UT) with 10% FBS (HyClone, Logan, UT), 100 U/ml penicillin, and 100 mg/ml streptomycin. Peritoneal macrophages were maintained at 37°C in a humidified atmosphere containing 5% CO_2. Nonadherent cells were removed after the cells firmly adhered to culture dishes.

qRT-PCR analysis. Total RNA was isolated from RAW 264.7 macrophages, mouse peritoneal macrophages, and SVCs using Isol-RNA lysis reagent (5 Prime, Hamburg, Germany). cDNA was synthesized using Moloney murine leukemia virus (M-MuLV) reverse transcriptase (Fermentas, Glen Burnie, MD). For quantitative reverse transcription-PCR (qRT-PCR) reactions, the amplification was performed with SYBR green for 35 cycles of 95°C for 30 s, 58°C for 30 s, and 72°C for 30 s, followed by a final extension at 72°C for 5 min. The primers were designed and synthesized by Bioneer (Daejeon, South Korea), and the primer sequences are shown in Table S1 in the supplemental material.

Measurement of cellular nitrate and ROS levels. Nitrite was measured using the Griess reaction (20). Culture media (100 μl) were collected and incubated with an equal volume of Griess reagent for 10 min at room temperature. The nitrite concentration was determined by the absorbance at 550 nm, using sodium nitrite as a standard. Cellular ROS was measured using chloromethyl-2′,7′-dichlorodihydrofluorescein diacetate (chloromethyl-H_2DCFDA) (Invitrogen, Grand Island, NY). RAW 264.7 macrophages and peritoneal macrophages were incubated with DCFDA in the dark for 20 min and washed with PBS. Cells were detached from culture dishes and suspended in ice-cold PBS for fluorescence measurement using flow cytometry (BD Bioscience, San Jose, CA).

Measurement of cytokine secretion. Secretion of IL-6 and MCP-1 into conditioned medium was measured with an enzyme-linked immunosorbent assay (ELISA) according to the manufacturer's instructions (BioSource, Grand Island, NY).

Western blot analysis. Western blot analysis was performed as previously described (21), with a minor modification. The cells were lysed with TGN buffer (50 mM Tris, pH 7.5, 150 mM NaCl, 1% Tween 20, 0.2% NP-40, and protease inhibitor cocktail [GenDepot, Houston, TX]) and subjected to Western blotting. Equal amounts of protein (50 μg) were separated on SDS-PAGE gels and transferred to polyvinylidene difluoride (PVDF) membranes. The blots were blocked with 5% nonfat milk in TBST (25 mM Tris, pH 8.0, 137 mM NaCl, 2.7 mM KCl, and 0.1% Tween 20) at room temperature for 30 min, followed by overnight incubation with primary antibodies at 4°C. After washing 3 times with TBST, the blots were hybridized with horseradish peroxidase-conjugated secondary antibodies (Bio-Rad, Hercules, CA) in 5% nonfat milk dissolved in TBST at room temperature for 2 h and washed 3 times with TBST. The results were visualized with enhanced chemiluminescence. G6PD and β-actin antibodies were purchased from Sigma (St. Louis, MO); phospho-AKT, phospho-glycogen synthase kinase 3β (phospho-GSK3β), phospho-JNK, and phospho-ERK antibodies were purchased from Cell Signaling Technology (Danvers, MA); AKT, GSK3β, and phospho-p38 MAPK antibodies were purchased from BD Bioscience (San Jose, CA); and iNOS, p38 MAPK, ERK, and JNK antibodies were purchased from Santa Cruz Biotechnology (Santa Cruz, CA).

Adenovirus infection. G6PD adenovirus (Ad-G6PD) was produced by Neurogenex (Seoul, South Korea). G6PD cDNA was fused in frame with a FLAG epitope tag at its NH_2 terminus, which was cloned into an adenoviral vector, pEntrBHRNX. An empty adenovirus vector (Ad-mock) was used as control. For adenoviral infection, primary macrophages were incubated with serum-free DMEM and adenovirus for 12 h at 37°C. Then, the culture medium was replaced with fresh medium. Each experiment was performed 48 h after viral infection.

Transfection with DNA and siRNA. DNA and small interfering RNA (siRNA) were delivered into RAW 264.7 macrophages using electroporation, and then the experiments were conducted at least 24 h after transfection. Mouse G6PD cDNA was cloned into pcDNA3.1 (Invitrogen, Grand Island, NY). The sequences of the siRNAs targeting G6PD (siG6PD) and the p50 subunit of NF-κB (siNF-κB p50) are provided in Table S2 in the supplemental material. As a negative control, siGFP or siNC, neither of which has a target sequence in the mouse genome, was used for transfection experiments.

Conditioned-medium experiment. RAW 264.7 macrophages were transfected with enhanced green fluorescent protein (EGFP) or G6PD expression vector, and conditioned media were collected 24 h after transfection. Fully differentiated 3T3-L1 adipocytes were incubated with conditioned media for 24 h and stimulated with insulin (100 nM) for 30 min.

Analysis of human fat tissue. The present study was performed in accordance with the Declaration of Helsinki and was approved by the Ethical Committee on Human Research of Kyoto University Graduate School of Medicine (2004; no. 553). Signed informed consent was obtained from all subjects. Seventy Japanese subjects (32 men and 38 women; ages, 47 ± 1.9 years; body mass index [BMI], 28 ± 1.0 kg/m^2 [range, 18 to 55 kg/m^2]) were recruited for the study. Among the subjects, 41 with a BMI of 24 to 55 kg/m^2 were admitted to the Division of Endocrinology and Metabolism of Kyoto University Hospital for the treatment of obesity, hypertension, dyslipidemia, or type 2 diabetes mellitus. Waist circumference was measured at the umbilicus in an upright position. Blood samples were obtained at 0800 h after fasting overnight and 3 days before the adipose tissue biopsies. Subcutaneous- and visceral-fat areas were evaluated at the umbilical level by computerized tomography ($n = 33$) (Toshiba Medical Systems, Tokyo, Japan). Subcutaneous abdominal adipose tissue (SAT) biopsies were done in the morning after breakfast. The SAT (~2 g) was removed from the periumbilical region under local anesthesia (1% lidocaine). Samples were immediately frozen in liquid nitrogen and stored at −80°C until use.

Whole-mount immunohistochemistry. Mice were anesthetized by an intramuscular injection of a combination of anesthetics. After fixation by vascular perfusion of 1% paraformaldehyde in PBS, adipose tissues were isolated. The whole-mount tissues were then incubated for 1 h at room temperature with a blocking solution containing 5% goat serum (Jackson ImmunoResearch) in 0.3% PBS-Tween (PBST). After blocking, the whole-mount tissues were incubated overnight at 4°C with antibodies against F4/80 (clone Cl:A3-1, diluted 1:1,000; Serotec) and G6PD (diluted 1:500; Bethyl). After several washes with PBST, the whole-mount tissues were incubated for 1 h at room temperature with secondary antibodies, namely, Cy3- or Cy5-conjugated anti-rat antibody or anti-rabbit antibody (diluted 1:500; Jackson ImmunoResearch). The signals were visualized, and digital images were obtained using a Zeiss ApoTome microscope and a Zeiss LSM510 confocal microscope equipped with argon and helium-neon lasers (Carl Zeiss).

Luciferase assay. An NF-κB–luciferase reporter gene and EGFP or G6PD were cotransfected into RAW 264.7 macrophages by electroporation. After transfection, each group was treated with DHEA, 6-AN, or SB 203580 for 24 h. Luciferase assays were performed, and the results are expressed as relative luciferase units (luciferase activity/μg protein).

RESULTS

Macrophage G6PD expression is higher in obese subjects. Previously, we reported that G6PD expression is elevated in the adipose tissue of obese and diabetic *db/db* mice (17). To investigate whether the level of G6PD expression in ATMs is correlated with adiposity, G6PD mRNA levels were measured in the SVC fractions of epididymal fat tissues from obese-mouse models, such as HFD-fed mice and *db/db* mice. Compared to lean mice, obese mice had higher levels of G6PD mRNA in the SVC fractions of fat tissue (Fig. 1A and B). In addition, to examine the level of G6PD protein in ATMs, we stained SVC fractions from lean *db/+* or obese *db/db* mice with fluorescence-labeled antibodies against macrophage marker (CD11b and F4/80) and G6PD. By flow cytometry, CD11b and F4/80 double-positive cells were selected to measure the level of G6PD protein. As shown in Fig. 1C, the level of ATM G6PD protein was higher in *db/db* mice than in *db/+* mice. To confirm this, we also performed whole-tissue immunohistochemistry. Compared to lean mice, G6PD-positive signals were enhanced and were colocalized with CD11b-positive macrophages in the adipose tissue of *db/db* mice (Fig. 1D). Similarly, G6PD was also increased and colocalized with macrophage marker in HFD-fed obese mice compared to NCD-fed lean mice (see Fig. S1 in the supplemental material). When G6PD expression was analyzed in human adipose tissue, the levels of G6PD mRNA were positively correlated with several indices of obesity—BMI, waist circumference, and visceral-fat area—but not subcutaneous-fat area, which is rarely associated with metabolic diseases (Fig. 1E). In addition, insulin resistance, assessed by the insulin resistance index (IRI) and the homeostasis model assessment for insulin resistance (HOMA-IR), was positively correlated with the level of adipose G6PD mRNA (Fig. 1F). Moreover, the mRNA levels of macrophage marker genes (CD68 and MAC1) and MCP-1 were positively correlated with the level of G6PD mRNA in human fat tissue (Fig. 1G). These results indicate that G6PD expression is increased in the ATMs of obese subjects with insulin resistance.

LPS and FFAs stimulate macrophage G6PD expression. Expression of hepatic G6PD has been shown to be sensitively regulated by nutritional and hormonal states (22). However, the specific stimuli responsible for the upregulation of macrophage G6PD in obesity have not been clearly addressed. To tackle this, RAW 264.7 macrophages were challenged with various stimuli associated with metabolic disorders, and the levels of G6PD mRNA and protein were examined by quantitative real-time PCR and Western blot analyses, respectively. In macrophages, FFAs and LPS augmented the levels of G6PD mRNA and protein, concomitant with increased proinflammatory cytokines, such as IL-6, MCP-1, TNF-α, and iNOS, which are known to sensitively respond to both stimuli, FFAs and LPS (Fig. 2A to D). Similarly, G6PD expression was elevated by FFA in primary macrophages (see Fig. S2 in the supplemental material). In contrast, large amounts of glucose or insulin did not alter G6PD expression in macrophages (see Fig. S3 in the supplemental material). These results imply that increase of macrophage G6PD in obesity might be induced by FFAs and LPS, which are also elevated in obese animals. Unlike G6PD, other cytosolic NADPH-producing enzymes, including isocitrate dehydrogenase 1 (IDH1) and malic enzyme 1 (ME1), were not significantly increased in macrophages by LPS (Fig. 2E), suggesting that G6PD might be a key NADPH-producing enzyme that links extracellular stimuli with the inflammatory cascade in macrophages.

Macrophage G6PD regulates the expression of proinflammatory cytokines. To characterize the roles of macrophage G6PD, the effects of G6PD activation and inhibition on proin-

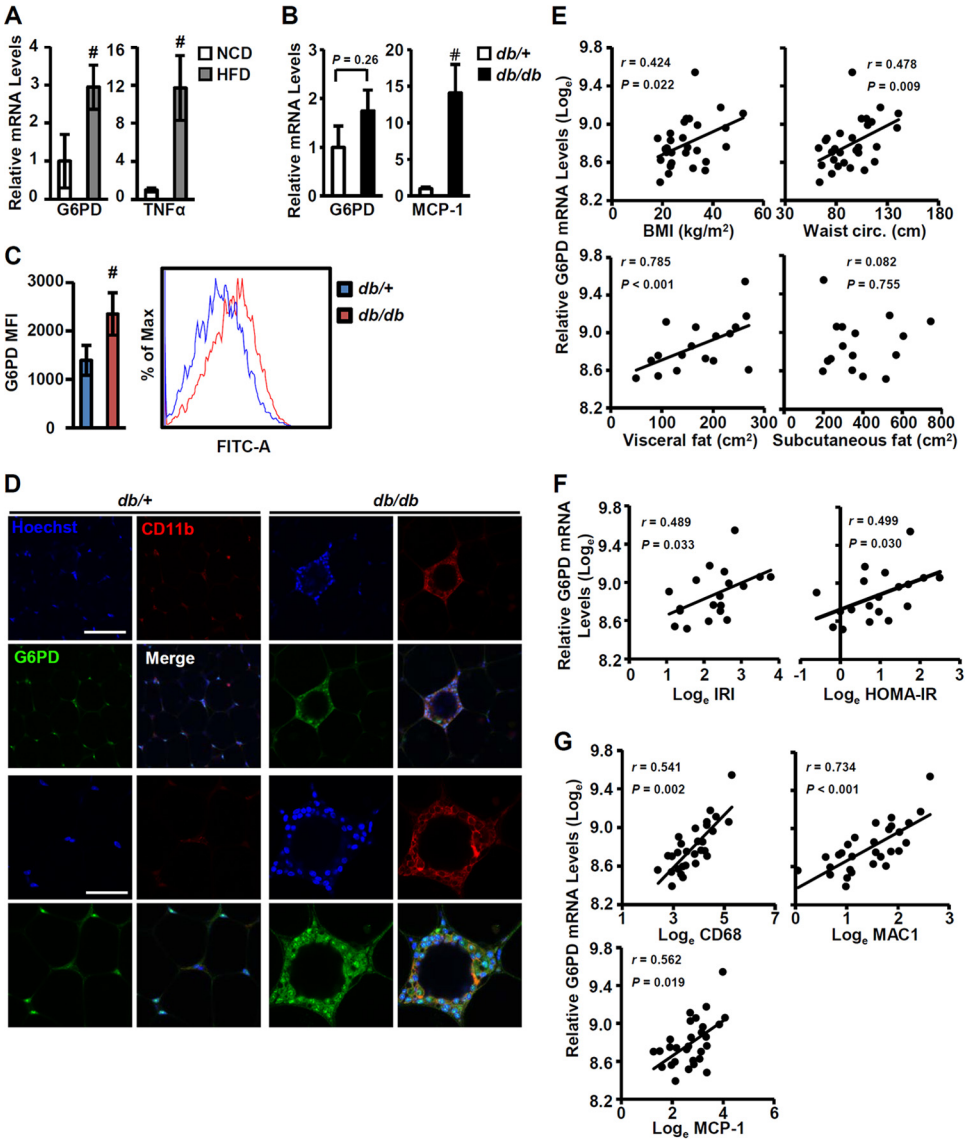

FIG 1 G6PD is increased in ATMs of obese animals. (A and B) Relative levels of G6PD mRNA in SVC fractions from fat tissues of NCD-fed lean mice and HFD-fed obese mice (A) and *db/+* and *db/db* mice (B). TNF-α and MCP-1 mRNA was evaluated as a positive control. The values shown are normalized to the levels of GAPDH mRNA and are reported as the mean ± standard deviation (SD). #, $P < 0.01$ versus NCD or *db/+* by Student's *t* test. (C) Expression levels of G6PD in ATMs of lean *db/+* and obese *db/db* mice. Intracellular G6PD was stained with fluorescein isothiocyanate (FITC)-conjugated antibody (FITC-A), and the fluorescence intensity was measured using flow cytometry. The G6PD mean fluorescence intensity (MFI) is reported as the mean ± SD. #, $P < 0.01$ versus *db/+* by Student's *t* test. One representative histogram per group is shown. (D) Expression pattern of G6PD protein in adipose tissue of lean *db/+* and obese *db/db* mice. Whole-mount immunohistochemistry analysis for the nucleus (Hoechst; blue), CD11b (red), and G6PD (green) was performed on the gonadal fat tissues of *db/+* and *db/db* mice. Bars = 100 μm (upper) and 50 μm (lower). (E to G) Relative levels of G6PD mRNA in human adipose tissues. (E) Correlation between G6PD and several indices of obesity (BMI, waist circumference, visceral-fat area, and subcutaneous-fat area). (F) Correlation between G6PD and indices of insulin resistance (IRI and HOMA-IR). (G) Correlation between G6PD and macrophage marker (CD68, MAC1, and MCP-1) genes.

flammatory responses were investigated. In macrophages, G6PD overexpression stimulated the expression of various proinflammatory cytokine genes, including IL-6, IL-1β, MCP-1, and TNF-α genes (Fig. 3A). Consistently, G6PD-overexpressing macrophages secreted high levels of IL-6 and MCP-1 (Fig. 3B). To confirm the effect of macrophage G6PD on proinflammatory cytokine gene expression, G6PD expression was suppressed with siRNA. In G6PD-suppressed macrophages, both basal and LPS-induced IL-6 and MCP-1 mRNA expression was alleviated (Fig. 3C). In agreement with these results, when the enzymatic activity of G6PD was repressed by DHEA or 6-AN, LPS-induced expression of IL-6 and MCP-1 decreased significantly (Fig. 3D and E). These results indicate that macrophage G6PD modulates the expression of proinflammatory genes. Given that proinflammatory cytokines produced from macrophages repress insulin signaling in adipocytes (7, 8, 23, 24), we tested whether increase of macrophage G6PD might affect insulin signaling in adipocytes. As shown in Fig. 3F, conditioned media from G6PD-overexpressing macrophages decreased the phosphorylation of AKT and GSK3β in insulin-treated adipocytes. These results suggest that elevation of macro-

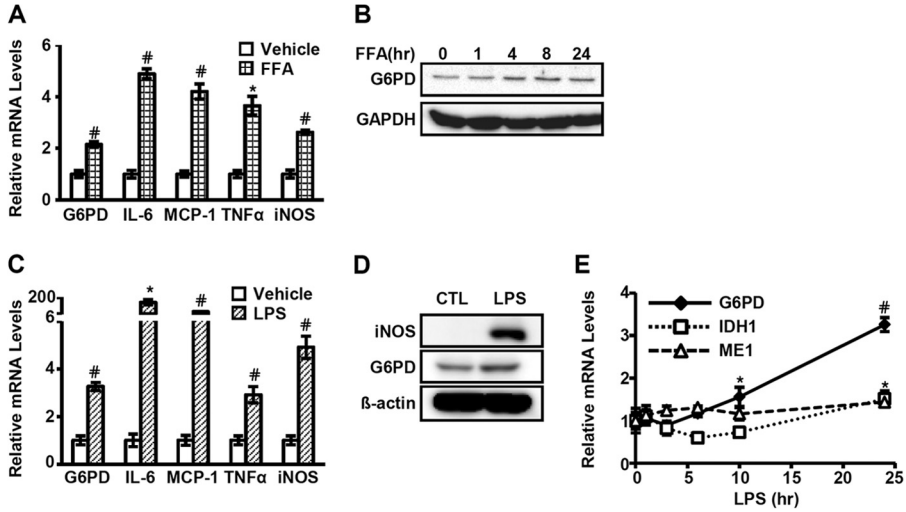

FIG 2 FFA and LPS stimulate G6PD expression in macrophages. (A and C) Induction of G6PD mRNA by treatment with FFA (palmitate) or LPS. RAW 264.7 macrophages were incubated with 100 μM palmitate (A) or 100 ng/ml of LPS (C) for 24 h. IL-6, MCP-1, TNF-α, and iNOS mRNAs were examined as positive controls. The values are normalized to the levels of cyclophilin mRNA and are reported as the mean ± SD. *, $P < 0.05$ versus vehicle; #, $P < 0.01$ versus vehicle (Student's *t* test). (B) Level of G6PD protein upon treatment with FFA (palmitate). RAW 264.7 macrophages were treated with palmitate (100 μM) for various times. (D) Expression of G6PD protein upon treatment with LPS. RAW 264.7 macrophages were incubated with 100 ng/ml of LPS for 24 h. CTL, negative control for the LPS group. iNOS was used as a positive control for LPS treatment. (E) mRNA levels of NADPH-producing genes, such as G6PD, IDH1, and ME1, upon treatment with LPS. Cells were treated with 100 ng/ml of LPS for various times. The values are normalized to the levels of cyclophilin mRNA and are reported as means ± SD. *, $P < 0.05$ versus 0 h; #, $P < 0.01$ versus 0 h (Student's *t* test).

phage G6PD would attenuate insulin sensitivity in adipocytes, probably through secretion of proinflammatory cytokines.

Macrophage G6PD augments oxidative stress. It has been well established that oxidative stress stimulates proinflammatory signaling cascades (14, 25). Given that G6PD produces NADPH, which plays a crucial role in the regulation of cellular redox, we asked whether the increase of proinflammatory gene expression in macrophages mediated by G6PD is associated with oxidative stress. To address this, we investigated the expression of ROS- and RNS-producing genes and their products. As shown in Fig. 4A, iNOS expression increased significantly in G6PD-overexpressing macrophages. To determine the enzymatic activity of iNOS, the level of nitrate, which is spontaneously generated from nitric oxide (NO), was examined in conditioned media. In accordance with the observed level of iNOS gene expression, the amount of nitrate was higher in G6PD-overexpressing macrophages than in control macrophages (Fig. 4B). Consistently, both basal and LPS-induced levels of iNOS mRNA were reduced in G6PD-suppressed macrophages (see Fig. S4 in the supplemental material). Moreover, the mRNA levels of NOX2 components (p40phox, p47phox, and p67phox) were also elevated by G6PD in macrophages (Fig. 4C). However, the mRNA levels of ROS-scavenging enzymes, such as catalase and superoxide dismutase, were not altered by G6PD (see Fig. S5 in the supplemental material). These results led us to propose the idea that the G6PD-mediated increase in ROS- and RNS-producing enzymes might confer cellular oxidative stress in macrophages. To test this, cellular ROS levels were determined using a fluorescent dye. As shown in Fig. 4D, the basal level of cellular ROS was increased by G6PD in primary macrophages. In addition, stimulation with hydrogen peroxide further augmented the level of cellular ROS in G6PD-overexpressing primary macrophages. In contrast, suppression of G6PD expression by siRNA reduced the level of cellular ROS in hydrogen peroxide-treated RAW 264.7 macrophages (Fig. 4E). In these experiments, hydrogen peroxide did not affect the viability of primary macrophages and RAW 264.7 macrophages (see Fig. S6 in the supplemental material). These results imply that augmentation of G6PD would confer oxidative stress in macrophages.

In macrophages, ROS and RNS are important signaling molecules that promote various signal transduction pathways linked to proinflammatory responses (10, 11, 14, 26). To elucidate the potential roles of ROS in G6PD-induced proinflammatory gene expression, macrophages were treated with the antioxidant NAC, and the level of MCP-1, a representative proinflammatory gene, was examined. As shown in Fig. 4F, NAC decreased the levels of MCP-1 mRNA in both control and G6PD-overexpressing macrophages, implying that the increased oxidative stress mediated by macrophage G6PD stimulates proinflammatory gene expression.

NADPH mediates the effects of macrophage G6PD on proinflammatory gene expression. NADPH participates in the regulation of redox potential as one of the key redox pairs. To determine whether the NADPH produced by G6PD is involved in oxidative stress and proinflammatory responses in macrophages, macrophages were treated with NADPH. Treatment with NADPH increased the level of intracellular NADPH in macrophages (see Fig. S7 in the supplemental material). Further, NADPH elevated cellular ROS levels in macrophages (Fig. 5A) and modestly stimulated the expression of proinflammatory genes and ROS/RNS-producing genes (Fig. 5B). Therefore, these data indicate that the effects of macrophage G6PD on oxidative stress and proinflammatory responses are mediated, at least in part, by increased cellular NADPH.

p38 MAPK is activated by macrophage G6PD overexpression. It has been well established that oxidative stress in macrophages activates MAPK signaling cascades, which play an essential role in the regulation of gene expression (27). Although all 3

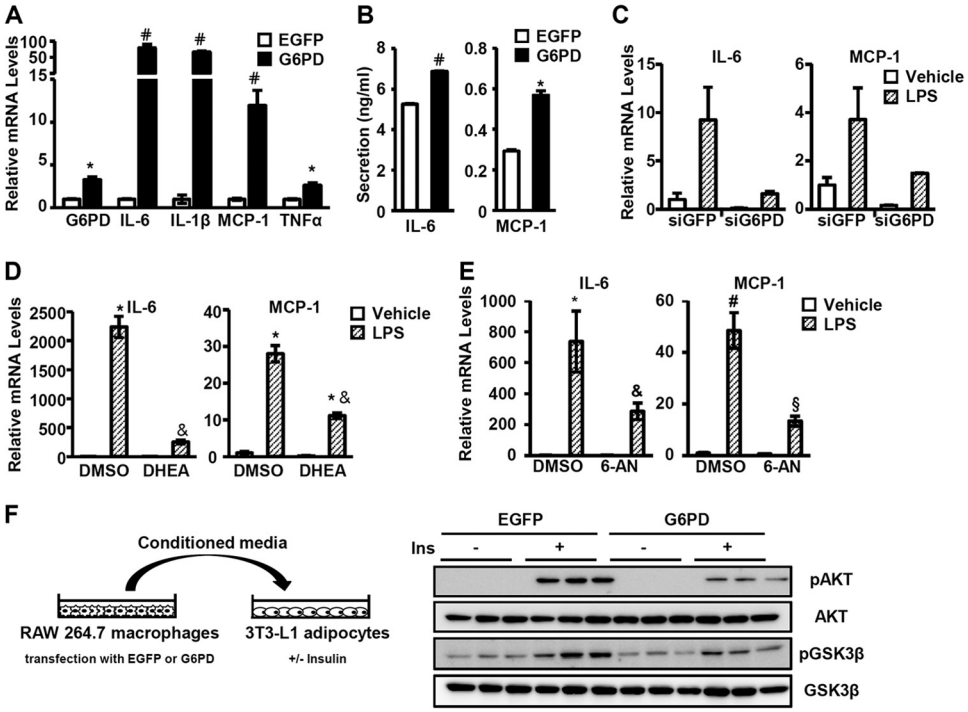

FIG 3 Macrophage G6PD modulates the expression of proinflammatory cytokines. (A) Levels of proinflammatory cytokine mRNAs in G6PD-overexpressing macrophages. RAW 264.7 macrophages were transfected with EGFP or G6PD, and then total RNA was isolated to analyze the expression of G6PD, IL-6, IL-1β, MCP-1, and TNF-α mRNAs by qRT-PCR. The values are normalized to the levels of cyclophilin mRNA and are reported as means ± SD. *, $P < 0.05$ versus EGFP; #, $P < 0.01$ versus EGFP (Student's *t* test). (B) Secretion of proinflammatory cytokines upon G6PD overexpression. Secreted IL-6 and MCP-1 cytokines were measured in conditioned media from EGFP- or G6PD-overexpressing RAW 264.7 macrophages. The results are reported as means + SD. *, $P < 0.05$ versus EGFP; #, $P < 0.01$ versus EGFP (Student's *t* test). (C) Levels of IL-6 and MCP-1 mRNAs in G6PD-suppressed macrophages. After transfection with siGFP or siG6PD, RAW 264.7 cells were challenged with LPS (100 ng/ml) for 3 h. The values are normalized to the levels of cyclophilin mRNA and are reported as means + SD. (D and E) Levels of IL-6 and MCP-1 mRNAs with or without G6PD inhibitors, such as DHEA (D) and 6-AN (E). Mouse peritoneal macrophages were incubated with or without G6PD inhibitors (DHEA, 100 μM; 6-AN, 100 μM) and/or LPS (100 ng/ml). The values are normalized to the levels of cyclophilin mRNA and are reported as means ± SD. *, $P < 0.05$ versus DMSO-vehicle; #, $P < 0.01$ versus DMSO-vehicle; &, $P < 0.05$ versus DMSO-LPS; §, $P < 0.01$ versus DMSO-LPS (Student's *t* test). (F) Insulin sensitivity in adipocytes treated with conditioned media from G6PD-overexpressing macrophages. RAW 264.7 macrophages were transfected with EGFP or G6PD expression vector, and then conditioned media were harvested. Fully differentiated 3T3-L1 adipocytes were treated with the conditioned media (24 h), followed by treatment with insulin (100 nM) for 30 min. Phosphorylation of AKT (S473) and GSK3β (S9) was detected using specific antibodies.

MAPKs (ERK, p38 MAPK, and JNK) are activated by ROS, specific MAPKs appear to be activated, depending on the stimuli or cell types (28–32). To understand the molecular mechanisms underlying macrophage G6PD-mediated regulation of inflammatory gene expression, we investigated whether macrophage G6PD affects MAPK activation. As shown in Fig. 6A, phosphorylation of p38 MAPK was evidently stimulated in G6PD-overexpressing macrophages, while phosphorylation of ERK and JNK was not altered. Furthermore, suppression of G6PD with siG6PD or DHEA obviously attenuated the phosphorylation of p38 MAPK when the cells were challenged with LPS (Fig. 6B and C). In addition, treatment with NADPH, an enzymatic product of G6PD, elevated the phosphorylation of p38 MAPK, and such increase was abolished by pretreatment with NAC in macrophages (see Fig. S8 in the supplemental material). To clarify the involvement of p38 MAPK in G6PD-induced proinflammatory gene expression, G6PD-overexpressing macrophages were treated with a p38 MAPK inhibitor, SB 203580. The expression of proinflammatory genes, such as the IL-6 and IL-1β genes, was significantly downregulated by SB 203580 (Fig. 6D), implying that p38 MAPK mediates the effects of G6PD on the expression of proinflammatory genes in macrophages.

Activation of NF-κB contributes to the expression of proinflammatory genes in G6PD-overexpressing macrophages. NF-κB is a key transcription factor that is activated by oxidative stress and governs the expression of most proinflammatory genes. To examine the effect of G6PD on NF-κB activation, we conducted luciferase reporter assays using NF-κB-responsive elements. As shown in Fig. 7A, G6PD overexpression in macrophages significantly stimulated the transcriptional activity of NF-κB. Furthermore, G6PD inhibitors, such as DHEA or 6-AN, attenuated the transcriptional activity of NF-κB. To verify the involvement of NF-κB in G6PD-induced proinflammatory gene expression, the activity of NF-κB was repressed with BAY 11-7082, an inhibitor of IκB phosphorylation. In macrophages, BAY 11-7082 reduced the levels of G6PD-induced IL-6 and MCP-1 mRNAs (Fig. 7B). Moreover, suppression of NF-κB p50 with siRNA greatly decreased the expression of proinflammatory genes and ROS/RNS-producing genes, which were upregulated by G6PD (Fig. 7C). Therefore, these data suggest that the increase of G6PD in macrophages activates the transcriptional activity of NF-κB, which leads to elevation of proinflammatory and oxidative-stress components in macrophages.

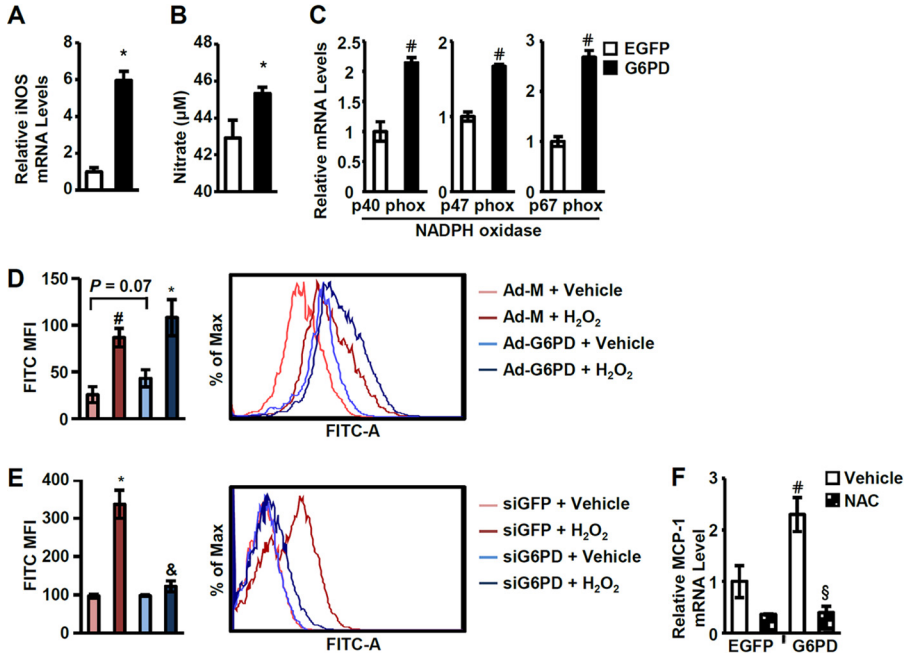

FIG 4 Macrophage G6PD regulates the expression of ROS- and RNS-producing genes and their products. (A) mRNA levels of iNOS in G6PD-overexpressing RAW 264.7 macrophages. The values are normalized to the levels of cyclophilin mRNA and are reported as means + SD. *, $P < 0.05$ versus EGFP by Student's *t* test. (B) Level of nitric oxide in G6PD-overexpressing macrophages. Conditioned media from EGFP- or G6PD-overexpressing macrophages were used to measure nitrate concentrations. The results are reported as means + SD. *, $P < 0.05$ versus EGFP by Student's *t* test. (C) mRNA levels of subunits of NADPH oxidase (p40phox, p47phox, and p67phox) in G6PD-overexpressing RAW 264.7 macrophages. The values are normalized to the levels of cyclophilin mRNA and are reported as means ± SD. #, $P < 0.01$ versus EGFP by Student's *t* test. (D) Cellular ROS levels upon G6PD overexpression. After infection with Ad-mock (Ad-M) or Ad-G6PD, peritoneal macrophages were treated with hydrogen peroxide (100 μM) for 20 min. The cells were then incubated with the redox-sensitive fluorescent dye chloromethyl-H_2DCFDA for 10 min. The fluorescence intensity was measured using flow cytometry. The results are reported as means ± SD. *, $P < 0.05$ versus vehicle; #, $P < 0.01$ versus vehicle (Student's *t* test). One representative histogram per group is shown. (E) Cellular ROS levels in G6PD-suppressed (siRNA) macrophages. After transfection with siGFP or siG6PD, RAW 264.7 macrophages were treated with hydrogen peroxide (100 μM) for 20 min. The results are reported as means ± SD. *, $P < 0.05$ versus vehicle; &, $P < 0.05$ versus siGFP (Student's *t* test). One representative histogram per group is shown. (F) Level of MCP-1 mRNA after treatment with antioxidant. After transfection with EGFP or G6PD, cells were treated with NAC (20 mM) for 24 h. The results are reported as means ± SD. #, $P < 0.01$ versus EGFP; §, $P < 0.01$ versus vehicle (Student's *t* test).

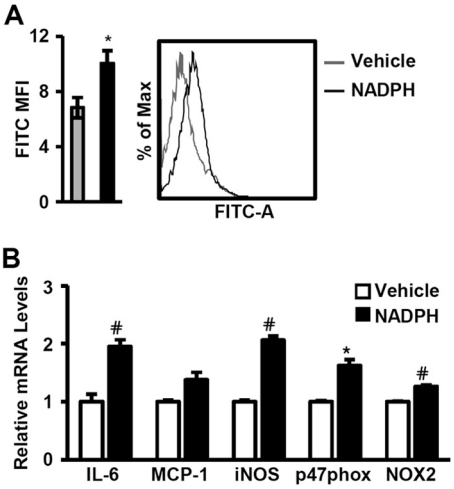

FIG 5 NADPH mediates the effect of G6PD on ROS production and proinflammatory gene expression. (A) ROS accumulation in NADPH-treated RAW 264.7 macrophages. RAW 264.7 macrophages were treated with NADPH (100 μM) for 24 h. The results are reported as means ± SD. *, $P < 0.05$ versus vehicle by Student's *t* test. One representative histogram per group is shown. (B) Levels of proinflammatory and ROS-producing genes in NADPH-treated RAW 264.7 macrophages. The cells were treated with NADPH (100 μM) for 24 h. The values are normalized to the levels of cyclophilin mRNA and are reported as means + SD. *, $P < 0.05$ versus vehicle; #, $P < 0.01$ versus vehicle (Student's *t* test).

DISCUSSION

In obese animals, adipose tissues exhibit chronic and low-grade inflammation, which is a key contributor to various metabolic disorders, such as insulin resistance, type 2 diabetes, cardiovascular disease, and atherosclerosis. Recent data have suggested that dysregulation of several metabolites and their signaling pathways is closely associated with inflammatory responses (3, 33). Here, we show that macrophage G6PD, an enzyme that regulates glucose flux, is elevated in the fat tissue of obese subjects and that macrophage G6PD promotes oxidative stress and proinflammatory responses, accompanied by p38 MAPK and NF-κB activation.

It has been proposed that G6PD could act as an antioxidative enzyme by producing NADPH, a key reducing cofactor for reduction of glutathione, which could alleviate oxidative stress (34–36). For instance, G6PD deficiency is a well-known human enzymopathy, which is characterized by hemolytic anemia due to increased susceptibility to oxidative stress in red blood cells (37). However, it is noteworthy that NADPH is also an essential cofactor for prooxidative enzymes that generate ROS and RNS. For example, it has been demonstrated that activation or overexpression of G6PD increases NO production in RINm5F rat insulinoma cells and bovine aortic endothelial cells (38, 39). Also, it has been reported that inhibition of G6PD decreases ROS and RNS in various cell types, including macrophages (40), granulocytes (20), and bovine

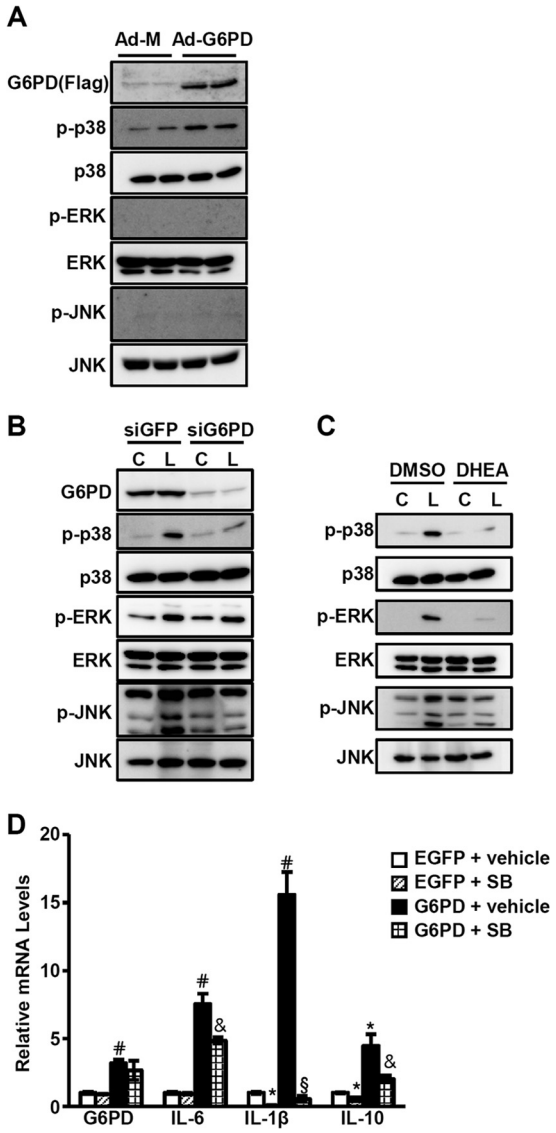

FIG 6 MAPK is involved in macrophage G6PD-induced inflammatory responses. (A) Phosphorylation of MAPKs, i.e., p38 MAPK (T180/Y182), ERK (T202/Y204), and JNK (T183/Y185), after overexpression of G6PD. After infection of peritoneal macrophages with adenovirus containing either Ad-mock or Ad-G6PD, phosphorylated (p-) or basal MAPKs were detected in total cell extracts. (B) Phosphorylation of MAPK after G6PD knockdown. After transfection of macrophages with GFP or G6PD siRNA, the cells were treated with LPS (L) (100 ng/ml) for 30 min and activation of MAPKs was compared to control (C). (C) Phosphorylation of MAPK with the G6PD inhibitor DHEA. RAW 264.7 macrophages were pretreated with DMSO or DHEA (100 μM) for 24 h and then treated with LPS (100 ng/ml) for 30 min. (D) Expression of proinflammatory genes in the presence or absence of p38 MAPK inhibitor (SB 203580). After transfection of RAW 264.7 macrophages with EGFP or G6PD, the cells were treated with either vehicle or SB 203580 (10 μM) for 24 h. The results are reported as means ± SD. *, $P < 0.05$ versus EGFP-vehicle; #, $P < 0.01$ versus EGFP-vehicle; &, $P < 0.05$ versus G6PD-vehicle; and §, $P < 0.01$ versus G6PD-vehicle (Student's *t* test).

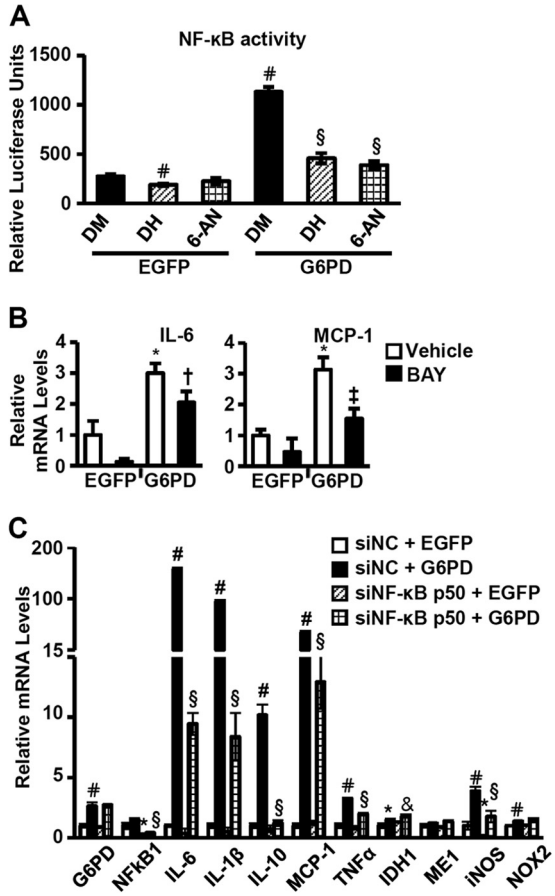

FIG 7 Macrophage G6PD activates NF-κB signaling. (A) Transcriptional activity of NF-κB with or without G6PD inhibitor treatment. An NF-κB–luciferase reporter was cotransfected into RAW 264.7 macrophages with EGFP or G6PD. After transfection, the cells were treated with DMSO (DM), DHEA (DH) (100 μM), or 6-AN (10 μM) for 24 h. The results are expressed in relative luciferase units (luciferase activity/μg protein) as means ± SD. #, $P < 0.01$ versus EGFP-DMSO; §, $P < 0.01$ versus G6PD-DMSO (Student's *t* test). (B) Expression of IL-6 and MCP-1 mRNAs after inhibition of NF-κB. After transfection of RAW 264.7 macrophages with EGFP or G6PD, the cells were treated with BAY 11-7082 (5 μM) for 24 h. The values are normalized to the levels of cyclophilin and are reported as means + SD. *, $P < 0.05$ versus EGFP-vehicle; †, $P = 0.11$ versus G6PD-vehicle; ‡, $P = 0.05$ versus G6PD-vehicle (Student's *t* test). (C) mRNA expression of several proinflammatory genes, NADPH-producing genes, and ROS/RNS-producing genes in NF-κB p50-suppressed (siRNA) macrophages. siRNA (siNC or siNF-κB p50) and expression vectors (EGFP or G6PD) were cotransfected into RAW 264.7 macrophages. The values are normalized to the levels of cyclophilin mRNA and are reported as means ± SD. *, $P < 0.05$ versus siNC-EGFP; #, $P < 0.01$ versus siNC-EGFP; &, $P < 0.05$ versus siNFKB1-EGFP; and §, $P < 0.01$ versus siNFKB1-EGFP (Student's *t* test).

colonary arteries (41). Therefore, it is very likely that the physiological roles of G6PD might be dependent on cell types that have distinct microenvironments, with different levels of pro-oxidative and antioxidative enzymes. In this study, we have demonstrated that macrophage G6PD increases cellular oxidative stress by elevation of ROS/RNS production, while knockdown or inhibition of G6PD decreases cellular ROS.

It has been reported that G6PD is involved in the inflammatory responses of several immune cells. For example, macrophages derived from G6PD-deficient mice exhibit more anti-inflammatory potential than those from wild-type (WT) mice (42). Also, mononuclear cells from G6PD-deficient patients secret fewer proinflammatory cytokines than those from normal subjects (43). Furthermore, severe G6PD deficiency resembles chronic granulomatous disease in that granulocytes from G6PD-deficient

patients have a defect in the respiratory burst responsible for killing bacteria in granulocytes (44–46). In line with these findings, in the present work, we report that increased G6PD expression in macrophages promotes proinflammatory signaling cascades by augmenting oxidative stress. Therefore, previous reports and our current findings imply that macrophage G6PD would potentiate proinflammatory responses.

Exposure to hydrogen peroxide or other stimuli that induce cellular ROS leads to activation of MAPKs (29), while prevention of ROS accumulation with antioxidants alleviates MAPK activation (47, 48), implying that MAPKs are key players in the propagation of oxidative stresses as a target of ROS. Although the mechanisms by which exogenously or endogenously produced ROS activates MAPKs are not yet thoroughly understood, several mechanisms have been proposed. In macrophages, we observed that G6PD selectively activated p38 MAPK, with slight activation of JNK or ERK. Interestingly, activation of p38 MAPK challenged with LPS was remarkably attenuated by suppression of G6PD via siRNA or DHEA. Furthermore, inhibition of p38 MAPK with SB 203580 repressed basal and G6PD-induced proinflammatory gene expression in macrophages. These results clearly suggest that activation of p38 MAPK plays a crucial role in macrophage G6PD-induced proinflammatory responses under pathophysiological stimuli.

In addition, we discovered that macrophage G6PD activated NF-κB, which was assessed by its transcriptional activity and target gene expression. NF-κB is a well-known master regulator of inflammatory responses (49). Previously, it has been reported that ROS promotes the transcriptional activity of NF-κB through several mechanisms, such as phosphorylation of RelA (12, 50) and activation of IκB kinase (IKK) (51). Although we observed that inhibition of NF-κB greatly suppressed G6PD-induced proinflammatory responses, we could not exclude the possibility that other transcription factors also contribute to G6PD-induced proinflammatory responses in macrophages. For instance, several transcription factors, such as Sp1, AP-1, p53, and HIF-1, have been reported to be redox-responsive transcription factors that appear to be differentially activated by oxidative stresses to exert proinflammatory responses (52, 53).

Various cellular signaling pathways influence each other through biochemical and physiological cross talk. For example, the p38 MAPK pathway plays a role in NF-κB activation (54–57). In this study, we revealed that macrophage G6PD activated p38 MAPK and NF-κB, while suppression or inhibition of macrophage G6PD reduced both of them. In addition, we observed that inhibition of p38 MAPK attenuated the transcriptional activity of NF-κB induced by macrophage G6PD (see Fig. S9 in the supplemental material). Taken together, these data suggest that G6PD-induced expression of proinflammatory cytokines might be mediated, at least in part, by p38 MAPK-dependent activation of NF-κB. Nevertheless, it is still plausible that macrophage G6PD-mediated activation of p38 MAPK and NF-κB constitutes a positive-feedback loop that amplifies proinflammatory responses.

Inflammatory diseases, including atherosclerosis (58), nonalcoholic steatohepatitis (59), and heart failure (60), deteriorate via vicious cycles between oxidative stress and inflammation. Similarly, it appears that a vicious cycle may play a role in the progression of dysregulated fat tissue in obese subjects, which commonly exhibits chronic and low-grade inflammation due to the accumulation of ATMs. Our data suggest that macrophage G6PD supplies NADPH to stimulate pro-oxidative enzymes, such as iNOS and NADPH oxidase, leading to increased cellular RNS and ROS. Then, ROS and RNS induce the expression of NF-κB-target genes, including ROS/RNS-producing enzymes and proinflammatory genes, which attenuate insulin signaling in adipocytes. Accordingly, we observed that knockdown of G6PD or treatment with G6PD inhibitors decreased cellular ROS and the expression of ROS/RNS-producing enzymes in macrophages. Therefore, it is reasonable to speculate that augmentation of macrophage G6PD might contribute to chronic and low-grade inflammatory signaling by accelerating a vicious cycle as follows: ROS/RNS→p38 MAPK→NF-κB→ROS/RNS-producing enzymes.

In the present study, we elucidated the pathophysiological roles of macrophage G6PD in obesity. Among the various environmental factors, FFAs and LPS promote G6PD expression in macrophages. Subsequent elevation of macrophage G6PD increases oxidative stress and activates p38 MAPK and NF-κB, which eventually stimulate proinflammatory genes and ROS/RNS-signaling cascades. Therefore, it appears that identifying the regulatory tools for macrophage G6PD could provide a promising treatment for inflammation- and/or oxidative-stress-linked metabolic diseases, such as obesity and type 2 diabetes.

ACKNOWLEDGMENTS

We thank Y. J. Koh and G. Y. Koh for their technical assistance with whole-mount immunohistochemistry.

This work was supported by grants from the Korea Science and Engineering Foundation funded by the South Korean government (Ministry of Education, Science, and Technology) (20120006079, 2012-0001241, and R31-10032). M.H., H.J., and G.C. were supported by BK21 Research Fellowships from the Ministry of Education and Human Resources Development.

We declare that we have no conflict of interest.

REFERENCES

1. **Kahn SE, Hull RL, Utzschneider KM.** 2006. Mechanisms linking obesity to insulin resistance and type 2 diabetes. Nature **444**:840–846.
2. **Lumeng CN, Saltiel AR.** 2011. Inflammatory links between obesity and metabolic disease. J. Clin. Invest. **121**:2111–2117.
3. **Shoelson SE, Lee J, Goldfine AB.** 2006. Inflammation and insulin resistance. J. Clin. Invest. **116**:1793–1801.
4. **Hotamisligil GS, Shargill NS, Spiegelman BM.** 1993. Adipose expression of tumor necrosis factor-alpha: direct role in obesity-linked insulin resistance. Science **259**:87–91.
5. **Ito A, Suganami T, Yamauchi A, Degawa-Yamauchi M, Tanaka M, Kouyama R, Kobayashi Y, Nitta N, Yasuda K, Hirata Y, Kuziel WA, Takeya M, Kanegasaki S, Kamei Y, Ogawa Y.** 2008. Role of CC chemokine receptor 2 in bone marrow cells in the recruitment of macrophages into obese adipose tissue. J. Biol. Chem. **283**:35715–35723.
6. **Kanda H, Tateya S, Tamori Y, Kotani K, Hiasa K, Kitazawa R, Kitazawa S, Miyachi H, Maeda S, Egashira K, Kasuga M.** 2006. MCP-1 contributes to macrophage infiltration into adipose tissue, insulin resistance, and hepatic steatosis in obesity. J. Clin. Invest. **116**:1494–1505.
7. **Weisberg SP, Hunter D, Huber R, Lemieux J, Slaymaker S, Vaddi K, Charo I, Leibel RL, Ferrante AW, Jr.** 2006. CCR2 modulates inflammatory and metabolic effects of high-fat feeding. J. Clin. Invest. **116**:115–124.
8. **Olefsky JM, Glass CK.** 2010. Macrophages, inflammation, and insulin resistance. Annu. Rev. Physiol. **72**:219–246.
9. **Aouadi M, Tesz GJ, Nicoloro SM, Wang M, Chouinard M, Soto E, Ostroff GR, Czech MP.** 2009. Orally delivered siRNA targeting macrophage Map4k4 suppresses systemic inflammation. Nature **458**:1180–1184.
10. **Gwinn MR, Vallyathan V.** 2006. Respiratory burst: role in signal transduction in alveolar macrophages. J. Toxicol. Environ. Health B Crit. Rev. **9**:27–39.
11. **Fialkow L, Wang Y, Downey GP.** 2007. Reactive oxygen and nitrogen

species as signaling molecules regulating neutrophil function. Free Radic. Biol. Med. **42**:153–164.
12. **Schreck R, Rieber P, Baeuerle PA.** 1991. Reactive oxygen intermediates as apparently widely used messengers in the activation of the NF-kappa B transcription factor and HIV-1. EMBO J. **10**:2247–2258.
13. **Lo YY, Cruz TF.** 1995. Involvement of reactive oxygen species in cytokine and growth factor induction of c-fos expression in chondrocytes. J. Biol. Chem. **270**:11727–11730.
14. **Forman HJ, Torres M.** 2001. Redox signaling in macrophages. Mol. Aspects Med. **22**:189–216.
15. **Emre Y, Nubel T.** 2010. Uncoupling protein UCP2: when mitochondrial activity meets immunity. FEBS Lett. **584**:1437–1442.
16. **Lambeth JD.** 2004. NOX enzymes and the biology of reactive oxygen. Nat. Rev. Immunol. **4**:181–189.
17. **Park J, Rho HK, Kim KH, Choe SS, Lee YS, Kim JB.** 2005. Overexpression of glucose-6-phosphate dehydrogenase is associated with lipid dysregulation and insulin resistance in obesity. Mol. Cell. Biol. **25**:5146–5157.
18. **Lee JW, Choi AH, Ham M, Kim JW, Choe SS, Park J, Lee GY, Yoon KH, Kim JB.** 2011. G6PD up-regulation promotes pancreatic beta-cell dysfunction. Endocrinology **152**:793–803.
19. **Park J, Choe SS, Choi AH, Kim KH, Yoon MJ, Suganami T, Ogawa Y, Kim JB.** 2006. Increase in glucose-6-phosphate dehydrogenase in adipocytes stimulates oxidative stress and inflammatory signals. Diabetes **55**: 2939–2949.
20. **Tsai KJ, Hung IJ, Chow CK, Stern A, Chao SS, Chiu DT.** 1998. Impaired production of nitric oxide, superoxide, and hydrogen peroxide in glucose 6-phosphate-dehydrogenase-deficient granulocytes. FEBS Lett. **436**:411–414.
21. **Kim KH, Yoon JM, Choi AH, Kim WS, Lee GY, Kim JB.** 2009. Liver X receptor ligands suppress ubiquitination and degradation of LXRalpha by displacing BARD1/BRCA1. Mol. Endocrinol. **23**:466–474.
22. **Salati LM, Amir-Ahmady B.** 2001. Dietary regulation of expression of glucose-6-phosphate dehydrogenase. Annu. Rev. Nutr. **21**:121–140.
23. **Hotamisligil GS, Arner P, Caro JF, Atkinson RL, Spiegelman BM.** 1995. Increased adipose tissue expression of tumor necrosis factor-alpha in human obesity and insulin resistance. J. Clin. Invest. **95**:2409–2415.
24. **Suganami T, Nishida J, Ogawa Y.** 2005. A paracrine loop between adipocytes and macrophages aggravates inflammatory changes: role of free fatty acids and tumor necrosis factor alpha. Arterioscler. Thromb. Vasc. Biol. **25**:2062–2068.
25. **Han CY, Umemoto T, Omer M, Den Hartigh LJ, Chiba T, LeBoeuf R, Buller CL, Sweet IR, Pennathur S, Abel ED, Chait A.** 2012. NADPH oxidase-derived reactive oxygen species increases expression of monocyte chemotactic factor genes in cultured adipocytes. J. Biol. Chem. **287**: 10379–10393.
26. **Kamata H, Hirata H.** 1999. Redox regulation of cellular signalling. Cell Signal. **11**:1–14.
27. **Torres M, Forman HJ.** 2003. Redox signaling and the MAP kinase pathways. Biofactors **17**:287–296.
28. **Gao D, Nong S, Huang X, Lu Y, Zhao H, Lin Y, Man Y, Wang S, Yang J, Li J.** 2010. The effects of palmitate on hepatic insulin resistance are mediated by NADPH oxidase 3-derived reactive oxygen species through JNK and p38MAPK pathways. J. Biol. Chem. **285**:29965–29973.
29. **Guyton KZ, Liu Y, Gorospe M, Xu Q, Holbrook NJ.** 1996. Activation of mitogen-activated protein kinase by H2O2. Role in cell survival following oxidant injury. J. Biol. Chem. **271**:4138–4142.
30. **Ishiyama J, Taguchi R, Yamamoto A, Murakami K.** 2010. Palmitic acid enhances lectin-like oxidized LDL receptor (LOX-1) expression and promotes uptake of oxidized LDL in macrophage cells. Atherosclerosis **209**: 118–124.
31. **Wang X, Martindale JL, Liu Y, Holbrook NJ.** 1998. The cellular response to oxidative stress: influences of mitogen-activated protein kinase signalling pathways on cell survival. Biochem. J. **333**:291–300.
32. **Yuan H, Zhang X, Huang X, Lu Y, Tang W, Man Y, Wang S, Xi J., Li J.** 2010. NADPH oxidase 2-derived reactive oxygen species mediate FFAs-induced dysfunction and apoptosis of beta-cells via JNK, p38 MAPK and p53 pathways. PLoS One **5**:e15726. doi:10.1371/journal.pone.0015726.
33. **Haschemi A, Kosma P, Gille L, Evans CR, Burant CF, Starkl P, Knapp B, Haas R, Schmid JA, Jandl C, Amir S, Lubec G, Park J, Esterbauer H, Bilban M, Brizuela L, Pospisilik JA, Otterbein LE, Wagner O.** 2012. The sedoheptulose kinase CARKL directs macrophage polarization through control of glucose metabolism. Cell Metab. **15**:813–826.
34. **Cosentino C, Grieco D, Costanzo V.** 2011. ATM activates the pentose phosphate pathway promoting anti-oxidant defence and DNA repair. EMBO J. **30**:546–555.
35. **Leopold JA, Zhang YY, Scribner AW, Stanton RC, Loscalzo J.** 2003. Glucose-6-phosphate dehydrogenase overexpression decreases endothelial cell oxidant stress and increases bioavailable nitric oxide. Arterioscler. Thromb. Vasc. Biol. **23**:411–417.
36. **Gaetani GD, Parker JC, Kirkman HN.** 1974. Intracellular restraint: a new basis for the limitation in response to oxidative stress in human erythrocytes containing low-activity variants of glucose-6-phosphate dehydrogenase. Proc. Natl. Acad. Sci. U. S. A. **71**:3584–3587.
37. **Frank JE.** 2005. Diagnosis and management of G6PD deficiency. Am. Fam Physician **72**:1277–1282.
38. **Guo L, Zhang Z, Green K, Stanton RC.** 2002. Suppression of interleukin-1 beta-induced nitric oxide production in RINm5F cells by inhibition of glucose-6-phosphate dehydrogenase. Biochemistry **41**:14726–14733.
39. **Leopold JA, Walker J, Scribner AW, Voetsch B, Zhang YY, Loscalzo AJ, Stanton RC, Loscalzo J.** 2003. Glucose-6-phosphate dehydrogenase modulates vascular endothelial growth factor-mediated angiogenesis. J. Biol. Chem. **278**:32100–32106.
40. **Hothersall JS, Gordge M, Noronha-Dutra AA.** 1998. Inhibition of NADPH supply by 6-aminonicotinamide: effect on glutathione, nitric oxide and superoxide in J774 cells. FEBS Lett. **434**:97–100.
41. **Gupte SA, Arshad M, Viola S, Kaminski PM, Ungvari Z, Rabbani G, Koller A, Wolin MS.** 2003. Pentose phosphate pathway coordinates multiple redox-controlled relaxing mechanisms in bovine coronary arteries. Am. J. Physiol. Heart Circ. Physiol. **285**:H2316–H2326.
42. **Wilmanski J, Siddiqi M, Deitch EA, Spolarics Z.** 2005. Augmented IL-10 production and redox-dependent signaling pathways in glucose-6-phosphate dehydrogenase-deficient mouse peritoneal macrophages. J. Leukoc. Biol. **78**:85–94.
43. **Sanna F, Bonatesta RR, Frongia B, Uda S, Banni S, Melis MP, Collu M, Madeddu C, Serpe R, Puddu S, Porcu G, Dessi S, Batetta B.** 2007. Production of inflammatory molecules in peripheral blood mononuclear cells from severely glucose-6-phosphate dehydrogenase-deficient subjects. J. Vasc. Res. **44**:253–263.
44. **Roos D, van Zwieten R, Wijnen JT, Gomez-Gallego F, de Boer M, Stevens D, Pronk-Admiraal CJ, de Rijk T, van Noorden CJ, Weening RS, Vulliamy TJ, Ploem JE, Mason PJ, Bautista JM, Khan PM, Beutler E.** 1999. Molecular basis and enzymatic properties of glucose 6-phosphate dehydrogenase volendam, leading to chronic nonspherocytic anemia, granulocyte dysfunction, and increased susceptibility to infections. Blood **94**:2955–2962.
45. **van Bruggen R, Bautista JM, Petropoulou T, de Boer M, van Zwieten R, Gomez-Gallego F, Belohradsky BH, Hartwig NG, Stevens D, Mason PJ, Roos D.** 2002. Deletion of leucine 61 in glucose-6-phosphate dehydrogenase leads to chronic nonspherocytic anemia, granulocyte dysfunction, and increased susceptibility to infections. Blood **100**:1026–1030.
46. **Cooper MR, DeChatelet LR, McCall CE, LaVia MF, Spurr CL, Baehner RL.** 1972. Complete deficiency of leukocyte glucose-6-phosphate dehydrogenase with defective bactericidal activity. J. Clin. Invest. **51**:769–778.
47. **Kyaw M, Yoshizumi M, Tsuchiya K, Kirima K, Tamaki T.** 2001. Antioxidants inhibit JNK and p38 MAPK activation but not ERK 1/2 activation by angiotensin II in rat aortic smooth muscle cells. Hypertens. Res. **24**: 251–261.
48. **Sekharam M, Cunnick JM, Wu J.** 2000. Involvement of lipoxygenase in lysophosphatidic acid-stimulated hydrogen peroxide release in human HaCaT keratinocytes. Biochem. J. **346**:751–758.
49. **Baker RG, Hayden MS, Ghosh S.** 2011. NF-kappaB, inflammation, and metabolic disease. Cell Metab. **13**:11–22.
50. **Nowak DE, Tian B, Jamaluddin M, Boldogh I, Vergara LA, Choudhary S, Brasier AR.** 2008. RelA Ser276 phosphorylation is required for activation of a subset of NF-kappaB-dependent genes by recruiting cyclin-dependent kinase 9/cyclin T1 complexes. Mol. Cell. Biol. **28**: 3623–3638.
51. **Kamata H, Manabe T, Oka S, Kamata K, Hirata H.** 2002. Hydrogen peroxide activates IkappaB kinases through phosphorylation of serine residues in the activation loops. FEBS Lett. **519**:231–237.
52. **Hui X, Li H, Zhou Z, Lam KS, Xiao Y, Wu D, Ding K, Wang Y, Vanhoutte PM, Xu A.** 2010. Adipocyte fatty acid-binding protein modulates inflammatory responses in macrophages through a positive feedback loop involving c-Jun NH2-terminal kinases and activator protein-1. J. Biol. Chem. **285**:10273–10280.

53. **Nishi K, Oda T, Takabuchi S, Oda S, Fukuda K, Adachi T, Semenza GL, Shingu K, Hirota K.** 2008. LPS induces hypoxia-inducible factor 1 activation in macrophage-differentiated cells in a reactive oxygen species-dependent manner. Antioxid. Redox Signal. **10**:983–995.
54. **Beyaert R, Cuenda A, Vanden Berghe W, Plaisance S, Lee JC, Haegeman G, Cohen P, Fiers W.** 1996. The p38/RK mitogen-activated protein kinase pathway regulates interleukin-6 synthesis response to tumor necrosis factor. EMBO J. **15**:1914–1923.
55. **Craig R, Larkin A, Mingo AM, Thuerauf DJ, Andrews C, McDonough PM, Glembotski CC.** 2000. p38 MAPK and NF-kappa B collaborate to induce interleukin-6 gene expression and release. Evidence for a cytoprotective autocrine signaling pathway in a cardiac myocyte model system. J. Biol. Chem. **275**:23814–23824.
56. **Wang C, Deng L, Hong M, Akkaraju GR, Inoue J., Chen ZJ.** 2001. TAK1 is a ubiquitin-dependent kinase of MKK and IKK. Nature **412**:346–351.
57. **Zechner D, Craig R, Hanford DS, McDonough PM, Sabbadini RA, Glembotski CC.** 1998. MKK6 activates myocardial cell NF-kappaB and inhibits apoptosis in a p38 mitogen-activated protein kinase-dependent manner. J. Biol. Chem. **273**:8232–8239.
58. **Harrison D, Griendling KK, Landmesser U, Hornig B, Drexler H.** 2003. Role of oxidative stress in atherosclerosis. Am. J. Cardiol. **91**:7A–11A.
59. **Begriche K, Igoudjil A, Pessayre D, Fromenty B.** 2006. Mitochondrial dysfunction in NASH: causes, consequences and possible means to prevent it. Mitochondrion **6**:1–28.
60. **Khaper N, Bryan S, Dhingra S, Singal R, Bajaj A, Pathak CM, Singal PK.** 2010. Targeting the vicious inflammation-oxidative stress cycle for the management of heart failure. Antioxid. Redox Signal. **13**:1033–1049.